ISSN No: - 2456 - 2165

Analysis and Simulation of Coaxial Bragg Fiber Using Toolbox

Prof. Amit Kumar
Dept. of Electronics and Communication
Krishna Institue of Engineering & Technology
Ghaziabad (U.P), India

Poonam Yadav
Dept. of Electronics and Communication
Krishna Institue of Engineering & Technology
Ghaziabad (U.P), India

***Abstract*—**In this paper, the propagation characteristic plays an extremely very important role in optical fiber communication system. We have given the information of various fibers which are available in communication system. Further, after using the two different methods (Exact solution and TMM). We have computed the propagation characteristic of Bragg fiber.

Keywords*—Optical fiber, Photoniccrystalfiber; Braggfiber.*

I. INTRODUCTION

Optic fibers communication is a communication that uses light pulses to transfer information from one point to another through an optical fiber. The information transmitted is essentially digital information generated by telephone systems. The optical fibers are dielectric cylindrical waveguide made from low-loss materials, usually silicon dioxide. The core of the waveguide has a refractive index a little higher than that of the outer medium (cladding), that light pulses is guided along the axis of the fiber by total internal reflection [1]. The optical communication systems is optical communication systems a very high degree of complexity. The normally includes multiple signal channels, different topologies, nonlinear devices, and non-Gaussian noise sources, is highly complex and labor-intensive. Advanced software tools make the design and analysis of these systems quick and efficient [2]. The growing demand for commercial software for optical communication systems has led to the availability of a number of different software solutions. More popular of these the optic system software as we noted in [3, 4].

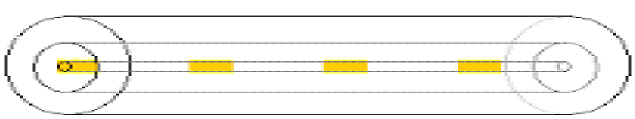

Figure1.1: Optical fiber

The Bragg fiber grating (FBG) [5] and extensive period grating [6] two of the most significant fiber filters and fiber sensor have been well advanced due to their advantages together with compression and fiber compatibility and numbers of applications. The photonic crystal fibers (PCFs) [7] which also Consist of Bragg fibers [8, 9] have attracted increasing importance over the past time because of their unique property.

Attention on the performance of photonic crystal fibers as useful components or devices as an alternate of a transmission medium. Photonic crystal fibers applications in fiber filters, fiber sensors, fiber lasers, and dispersion advantage have been well considered [10, 11]. Bragg fibers have in recent times received much attention for their motivating dispersion and modal properties and for advances in manufacture techniques [12]. Bragg fiber containing of a core bounded by alternating layers of small and great refractive index was first projected in [13]. Light is narrowed in the core by one dimensional photonic band gap. Bragg fiber is a beautiful knowledge, but it is relatively difficult to fabricate a Bragg fiber with square technique. It was more than 20 years later that first actual Bragg fiber is fabricated in MIT [14]. Which was composed of alternating layers of PES? A silica core Bragg fiber is fabricated by sputtering Si and SiO2 on the other hand on silica fiber [15], but the fiber length in only 20 cm, because the Si layers in cladding contains the drawing of fiber. An air-silica Bragg fiber design was recommended which was a cylindrically symmetric fiber with a high-index core (silica) enclosed by alternating layers of silica and air, dispersion properties of this air-silica Bragg fiber was discussed. It was impossible to arrange for structural support to this air-silica fiber, which made this design unrealizable. A Bragg fiber can also be calculated to a single guided mode without azimuthal dependence (TE or TM). In difference with the fundamental mode in conventional fiber which is always all the more degenerate, these guided Bragg fiber modes are really single mode. Therefore, many undesirable polarization dependent effects can be completely reduced in Bragg fiber [16].

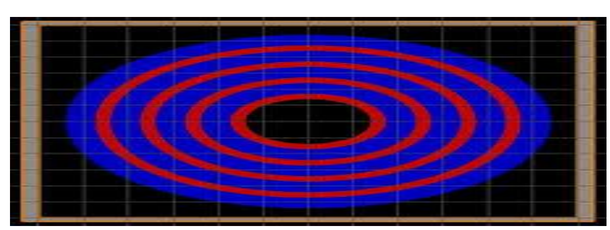

Figure 1.2: Bragg fibe

II. EXACT SOLUTION FOR STEP INDEX FIBERS

We will achieve the modal fields and the corresponding propagation numbers for step index fiber for which the refractive index variation is a fiber it is possible to achieve rigorous solutions of the vector equations. The most practical fibers used in communication are weakly guiding relative refractive index difference $(n_1 - n_2)/n_1 \ll 1$ and in such a case the radial part of the transverse element of the electric field satisfies the following

$$V(1-b)^{1/2}\frac{J_{l-1}\left(V(1-b)^{1/2}\right)}{J_l\left(V(1-b)^{1/2}\right)} = Vb^{1/2}\frac{K_{l-1}\left(V(b)^{1/2}\right)}{K_l\left(V(b)^{1/2}\right)}; l = \quad (1)$$

$$V(1-b)^{1/2}\frac{J_1\left(V(1-b)^{1/2}\right)}{J_0\left(V(1-b)^{1/2}\right)} = Vb^{1/2}\frac{K_1\left(V(b)^{1/2}\right)}{K_0\left(V(b)^{1/2}\right)}; \quad l = 0 \quad (2)$$

III. TRANSFER MATRIX METHO

We will present a matrix method near the compute the mode features as well as the power flux of radially stratified fibers. The simple idea is to replace the boundary conditions by a matrix equation. Thus, each cladding interface is characterized by a matrix. The intro diction of this 4 X 4 matrix greatly simplifies the analysis.

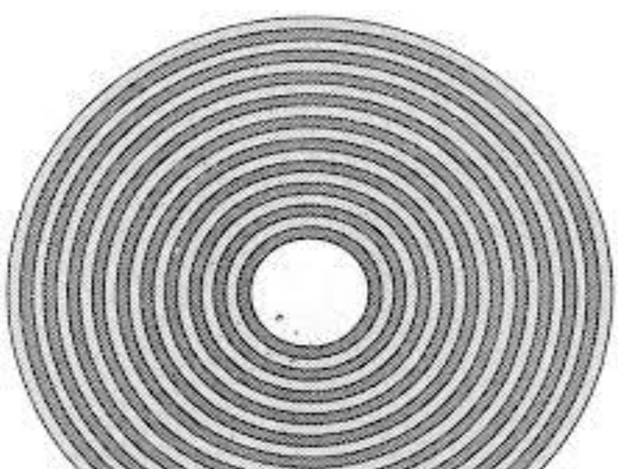

Fig.1.3: Bragg fiber

We study a fiber by the index profile given by

$$n(r) = \begin{cases} n_g & 0<r<r_1 \\ n_v, & r_v < r < r_{v+1} \\ & v = 1, 2, 3 \ldots \infty \end{cases} \quad (3)$$

In individual, we will study a fiber with a low index core then the alternating low and high index cladding. The geometry of this structure is drawn in Fig. 1.3. The index profile is then given by

$$n(r) = \begin{cases} n_g, & 0 \le r < r_1 \\ n_2, & r_1 \le r < r_2 \\ n_1, & r_2 \le r < r_3 \\ n_2, & r_3 \le r < r_4 \\ n_1, & r_4 \le r < r_5 \end{cases} \quad (4)$$

We income the z axis as the course of transmission, thus that every field factor has the form

$$\varphi(r,\theta,z,t) = \varphi(r,\theta)e^{i(\beta z-\omega t)} (5)$$

Where φ can be E_z, E_r, E_θ, H_r, H_θ, ω Is the angular frequency and β is the Spread constant.

From waveguide the transverse field components can be expert in terms of E_z and H_r

$$E_z = \frac{i\beta}{\omega^2\mu\epsilon-\beta^2}\left(\frac{\partial}{\partial r}Ez + \frac{\omega\mu}{\beta}\frac{\partial}{r\partial\theta}Hz\right) (6)$$

$$E_\theta = \frac{i\beta}{\omega^2\mu\epsilon-\beta^2}\left(\frac{\partial}{r\partial\theta}Ez - \frac{\omega\mu}{\beta}\frac{\partial}{\partial r}Hz\right) (7) \quad H_r = \frac{i\beta}{\omega^2\mu\epsilon-\beta^2}\left(\frac{\partial}{\partial r}Hz - \frac{\omega\epsilon}{\beta}\frac{\partial}{r\partial\theta}Ez\right) (8)$$

$$H_\theta = \frac{i\beta}{\omega^2\mu\epsilon-\beta^2}\left(\frac{\partial}{r\partial\theta}Hz + \frac{\omega\epsilon}{\beta}\frac{\partial}{\partial r}Ez\right) (9)$$

E_z (r,θ) $and\ Hz(r,\theta)\ satisfy\ the\ wave\ equation$

$$\nabla_t^2 + (\omega^2\mu\varepsilon - \beta^2)]\begin{Bmatrix} E_z \\ H_z \end{Bmatrix} = 0 (10)$$

Where $\nabla_t^2 = \nabla^2 - \frac{\partial^2}{\partial z^2}$ is the right angles operative.

The common solution can be written

E_z = [A J_l(kr) + B Y_l(kr)] $\cos(l\theta + \emptyset)$(11)

Hz = [C J_l(kr) + D Y_l(kr)] $\cos(l\theta + \varphi)$ (12)

Where A, B, C, D,$\emptyset$ and φ are numbers, l is an integer, and

K= $(\omega^2\mu\epsilon - \beta^2)^{1/2}$(13)

We at present study the boundary conditions at a common cladding interface at r = p. The result of the wave equation is taken as

ISSN No: - 2456 - 2165

E_z = [$A_1 J_l(k_1$r) + $B_1 Y_l(k_1$r)] cos($l\theta + \emptyset_1$), r< p

E_z= [$A_2 J_l(k_2$r) + $B_2 Y_l(k_2$r)] cos($l\theta + \emptyset_2$), r> p (14)

Or

H_z= [$C_1 J_l(k_1$r) + $D_1 Y_l(k_1$r)] cos($l\theta + \varphi_1$), r< p

H_z= [$C_2 J_l(k_2$r) + $D_2 Y_l(k_2 r)$] cos($l\theta + \varphi_2$), r> p (15)

Where
k_i = [($\omega/c)^2 \epsilon_i \mu_i$ -$\beta^2)^{1/2}$ i= 1, 2. (16)

The state line conditions at r = p are that E_z , H_z , E_z , E_θ are constant at the interface. Thus a 4×4 matrix can be start which relates A_1, B_1, C_1, D_1 to A_2, B_2, C_2, D_2

$$\begin{pmatrix} A_2 \\ B_2 \\ C_2 \\ D_2 \end{pmatrix} = M \begin{pmatrix} A_1 \\ B_1 \\ C_1 \\ D_1 \end{pmatrix} \quad (17)$$

1.1 Derivation of M

In relations of fields (14) and (15) the stability of E_z gives

[A J_l (k_1 p) + $B_1 Y_l(k_1 p)$] cos($l\theta + \emptyset_1$) = [$A_2 J_l$ (k_2 p) + $B_2 Y_l(k_2$p)]cos($l\theta + \emptyset_2$) (18)

This equation has to be content for all θ which denotes

$\emptyset_1 = \emptyset_2$(19)

They also from the continuity of H_z

$\varphi_1 = \varphi_2$(20)

Thus permanence of E_z *and* H_z *gives*

$A_1 J_l(k_1 p) + B_1 Y_l(k_1 p) = A_2 J_l(k_2 p) + B_2 Y_l(k_2 p)$(21)

$C_1 J_l(k_1 p) + D_1 Y_l(k_1 p) = C_2 J_l(k_2 p) + D_2 Y_l(k_2 p)$(22)

In relations of the field (14), (15) and (7), the stability of E_θ gives

$\frac{1}{k_1^2}(\frac{-l}{p}[A_1 J_l\ (k_1\text{p})\ + B_1 Y_l(k_1\text{p})]\sin(\ l\theta +\ \varphi)$-$\frac{\omega\mu_1}{\beta} k_1[C_1 J'_l(k_1 p) +$ $D_1 Y'_l(k_1 p)[\cos(\ l\theta + \varphi)$
= $\frac{1}{k_2^2}$ ($\frac{-l}{p}$ [$A_2 J_l$ ($k_2 p) + B_2 Y_l$ ($k_2 p)$] $\sin(\ l\theta +\ \emptyset)$ - $\frac{\omega\mu_2}{\beta} k_2[C_2 J'_l(k_2 p) +\ D_2 Y'_l(k_2$p)]cos($l\theta + \varphi$)(23)

Where up to date numbers the products with respect to their own disagreement. This equation has to be satisfied for all θ. From (21) and (22)

$(\frac{1}{k_1^2})\ [A_1 J_l(k_1 p) +\ B_1 Y_l(k_1 p)] \neq (\frac{1}{k_2^2})[A_2 J_l(k_2 p) +\ B_2 Y_l(k_2 p)]$
(24)
$(\frac{\mu_1}{k_1})[C_1 J'_l(k_1 p) +\ D_1 Y'_l(k_1 p)] \neq (\frac{\mu_2}{k_2})[C_2 J'_l(k_2 p) +\ D_2 Y'_l$p)]
(25)

In case $k_1 \neq k_2$. Thus we complete from (23)-(25) that

$\sin(\ l\theta +\ \emptyset) = \pm \cos(\ l\theta + \varphi)$(26)

Or

$\emptyset = \varphi \pm \frac{\pi}{2}$(27)

Continuity of H_θ and Eq. (9)

$\frac{1}{k_1^2}(\frac{-l}{p}[C_1 J_l\ (k_1\text{p})\ + D_1 Y_l(k_1\text{p})]\sin(\ l\theta +\ \varphi)$-$\frac{\omega\epsilon_1}{\beta} k_1[A_1 J'_l(k_1 p) +$ $B_1 Y'_l(k_1 p)[\cos(\ l\theta + \emptyset)]$
= $\frac{1}{k_2^2}$ ($\frac{-l}{p}$ [$C_2 J_l$ ($k_2 p) + D_2 Y_l$ ($k_2 p)$] $\sin(\ l\theta +\ \varphi)$ - $\frac{\omega\epsilon_2}{\beta} k_2[A_2 J'_l(k_2 p) +\ B_2 Y'_l(k_2$p)]cos($l\theta + \emptyset$)(28)

From (26) or (27) we categorize the waves into two types:

1. $E_z = [A\ \ J_l$(kr) + BY_l(kr)] cos $l\theta$

   H_z = [C J_l(kr) + D Y_l(kr)] sin $l\theta$(29)

2. E_z= [A J_l(kr) + B Y_l(kr)] sin $l\theta$(30)

   H_z = [C J_l(kr) + D Y_l(kr)] cos $l\theta$

The state line conditions for these two classifications

$A_1 J_l$ (k_1p) +$B_1 Y_l(k_1$p) + 0 + 0 = (1→ 2), (31)

$\frac{\omega\epsilon_1}{k_1\beta} A_1 J'_l(k_1 p) + \frac{\omega\epsilon_1}{k_1\beta} B_1 Y'_l(k_1 p)$ +$\frac{l}{k_1^2 p} C_1 J_l$ (k_1p) +$\frac{l}{k_1^2 p} D_1 Y_l(k_1$p) = (1 → 2) , (32)

0 + 0 + $C_1 J_l$ (k_1p) +$D_1 Y_l(k_1 p)$ = (1→ 2), (33)

$\frac{l}{k_1^2 p} A_1 J_l$ (k_1 p) + $\frac{l}{k_1^2 p} B_1 Y_l(k_1$p) + $\frac{\omega\mu_1}{k_1\beta} C_1 J'_l(k_1 p) +$ $\frac{\omega\mu_1}{k_1\beta} D_1 Y'_l(k_1 p)$ = (1→ 2), (34)

There are of the same kind equations except that the coefficient $\frac{l}{k_2^2 p}$ is replaced by $\frac{l}{k_1^2 p}$.Equations (31)-(34) can be written as a matrix equation.

$$M(1, p) = \begin{pmatrix} A_1 \\ B_1 \\ C_1 \\ D_1 \end{pmatrix} = M(2, P) \begin{pmatrix} A_2 \\ B_2 \\ C_2 \\ D_2 \end{pmatrix} \quad (35)$$

$$\begin{bmatrix} J_l(k_ip) & Y_l(k_ip) & 0 & 0 \\ \frac{\omega\epsilon_i}{\beta k_i}J'_l(k_ip) & \frac{\omega\epsilon_i}{\beta k_i}Y'_l(k_ip) & \frac{l}{k_i^2 p}J_l(k_ip) & \frac{l}{k_i^2 p}Y_l(k_ip) \\ 0 & 0 & J_l(k_ip) & Y_l(k_ip) \\ \frac{l}{k_i^2 p}J_l(k_ip) & \frac{l}{k_i^2 p}Y_l(k_ip) & \frac{\omega\mu_i}{\beta k_i}J'_l(k_ip) & \frac{\omega\mu_i}{\beta k_i}Y'_l(k_ip) \end{bmatrix}$$

(36)

Where i = 1, 2. We sign that when l = 0, the matrix is reducible we can have clean TE or pure TM waves when I = 0.

A matrix in Eq. (17) can be written as using (35),

$$M = M^{-1}(2, p)\, M(1, p) \quad (37)$$

If we define x $=k_1p, y = k_2p$, write M

$$M = \frac{\pi y}{2}\begin{pmatrix} m_{11} m_{12} m_{13} m_{14} \\ m_{21} m_{22} m_{23} m_{24} \\ m_{31} m_{32} m_{33} m_{34} \\ m_{41} m_{42} m_{43} m_{44} \end{pmatrix} \quad (38)$$

Using (36) and next some matrix use, the matrix elements m_{ij} in (38) are found as

$$m_{11} = J_l(x)Y'_l(y) - \left(\frac{k_{2\epsilon1}}{k_{1\epsilon2}}\right)J'_l(x)Y_l(y)$$

$$m_{12} = Y_l(x)Y'_l(y) - (k_{2\epsilon1}/k_{2\epsilon2})Y'_l(x)Y_l(y)$$

$$m_{13} = (\beta l/\omega\epsilon_2)(1/y - 1/x)\, J_l(x)Y_l(y)$$

$$m_{14} = (\beta l/\omega\epsilon_2)(1/y - 1/x)\, Y_l(x)Y_l(y)$$

$$m_{21} = \left(\frac{k_{2\epsilon1}}{k_{1\epsilon2}}\right)J_l'(x)J_l(y) - J_l(x)J'_l(y)$$

$$m_{22} = \left(\frac{k_{2\epsilon1}}{k_{1\epsilon2}}\right)Y'_l(x)J_l(y) - Y_l(x)J'_l(y)$$

$$m_{23} = (\beta l/\omega\epsilon_2)(1/x - 1/y)\, J_l(x)J_l(y)$$

$$m_{24} = (\beta l/\omega\epsilon_2)(1/x - 1/y)\, Y_l(x)J_l(y)$$

$$m_{31} = (\beta l/\omega\mu_2)(1/y - 1/x)\, J_l(x)Y_l(y)$$

$$m_{32} = (\beta l/\omega\mu_2)(1/y - 1/x)\, Y_l(x)Y_l(y)$$

$$m_{33} = J_l(x)Y'_l(y) - \left(\frac{k_{2\mu1}}{k_{1\mu2}}\right)J'_l(x)Y_l(y)$$

$$m_{34} = Y_l(x)Y'_l(y) - \left(\frac{k_{2\mu1}}{k_{1\mu2}}\right)Y'_l(x)Y_l(y)$$

$$m_{41} = (\beta l/\omega\mu_2)(1/x - 1/y)\, J_l(x)J_l(y)$$

$$m_{42} = (\beta l/\omega\mu_2)(1/x - 1/y)\, Y_l(x)J_l(y) \quad (39)$$

$$m_{43} = \left(\frac{k_{2\mu1}}{k_{1\mu2}}\right)J'_l(x)J_l(y) - J_l(x)J'_l(y)$$

$$m_{44} = \left(\frac{k_{2\mu1}}{k_{1\mu2}}\right)Y'_l(x)J_l(y) - Y_l(x)J'_l(y)$$

All over again we find that the transfer matrix M is block diagonal zed when l = 0. In this example the matrix equation (17) can be written as two single equations.

$$\begin{pmatrix} A_2 \\ B_2 \end{pmatrix} = M_{TM}\begin{pmatrix} A_1 \\ B_1 \end{pmatrix} (40)$$

$$\begin{pmatrix} C_2 \\ D_2 \end{pmatrix} = M_{TM}\begin{pmatrix} C_1 \\ D_1 \end{pmatrix} (41)$$

The matrix method described directly above can be employed to gain the mode dispersion relations for several conventional fibers.

IV. SIMULATION RESULTS

In this section we use the above method to analyze the propagation characteristics for a step index fiber. The Bessel equation has all the information that we can obtain from our modal analysis and it gives the result of this investigation. In this paper we have assume a step index fiber and consider a higher value of V (Let V=6.5 when n2 =1.45, Δ =0.0064, a =3 µm, and lambda = approx. 0.4757 µm) and plotted the LHS and RHS of equation (x) in fig4.1, 4.2, 4.3, 4.4, 4.5, 4.6, 4.7 (for l=0, 1, 2, 3, 4).We find that there are two modes corresponding to l=0 (also called LP $_{0X}$), two modes corresponding to l=1, and one mode each corresponding to l=2, 3 and l=4.

Table-1.1 Cutoff frequency of various linear polarized in a step index fiber

l	LP_{xx}	B
0	LP_{01}	0.8977
	LP_{02}	0.4752
1	LP_{10}	0.7422
	LP_{11}	0.1792
2	LP_{20}	0.5411
3	LP_{30}	0.3003
4	LP_{40}	0.0270
5	LP_{5x}	NA

The corresponding values of b are given in table-1.1. Further using the above method we have plotted in fig 4.6 the variation of the normalized propagation constant b with normalized frequency V for a step index fiber corresponding to some low order modes. From table-1.1 the smallest value of b is very close to cutoff frequency.

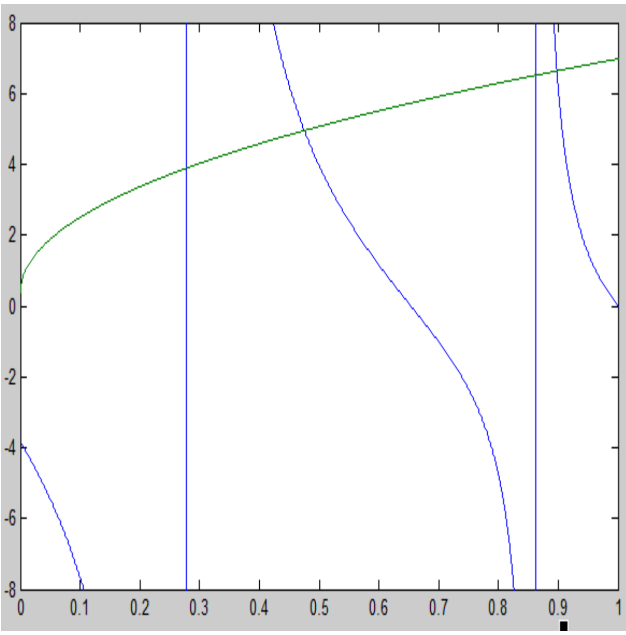

Figure 1.4:Variation of the LHS (blue color) and RHS (Green Color) in equation (1) and (2).This curve is plotted in case of l=0 and V=6.5. Also, the points of intersection represent the discrete modes of the waveguide.

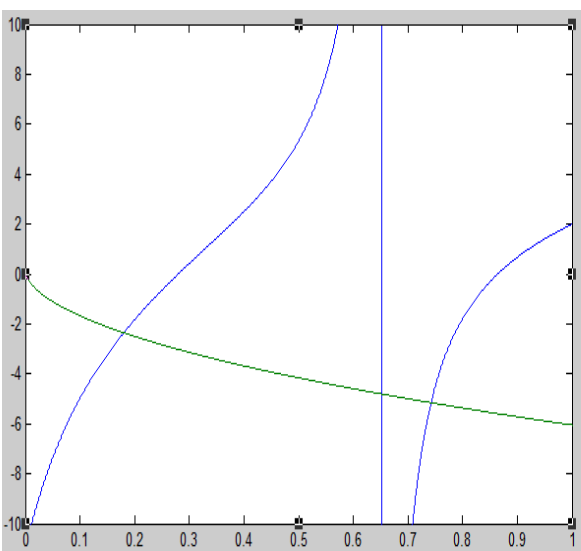

Figure 1.5:Variation of the LHS (blue color) and RHS (Green Color) in equation(1) and (2)This curve is plotted in case of l=1 and V=6.5. Also, the points of intersection represent the discrete modes of the waveguide.

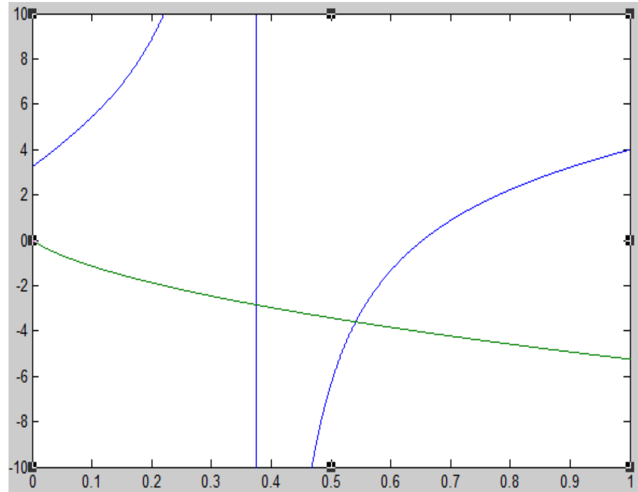

Figure 1.6:Variation of the LHS (blue color) and RHS (Green Color) in equation (1) and (2).This curve is plotted in case of l=2 and V=6.5. Also, the points of intersection represent the discrete modes of the waveguide.

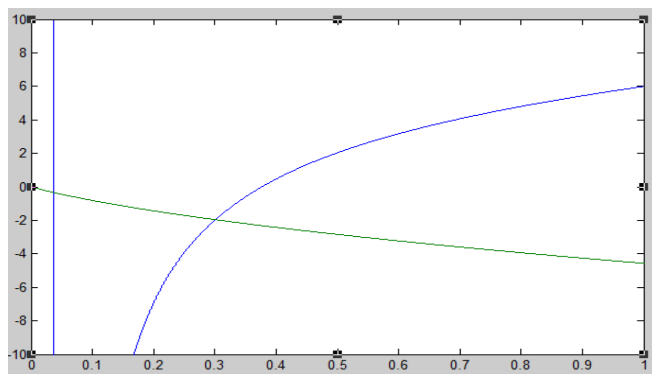

Figure 1.7:Variation of the LHS (blue color) and RHS (Green Color) in equation(1)and (2)This curve is plotted in case of l=3 and V=6.5. Also, the points of intersection represent the discrete modes of the waveguide.

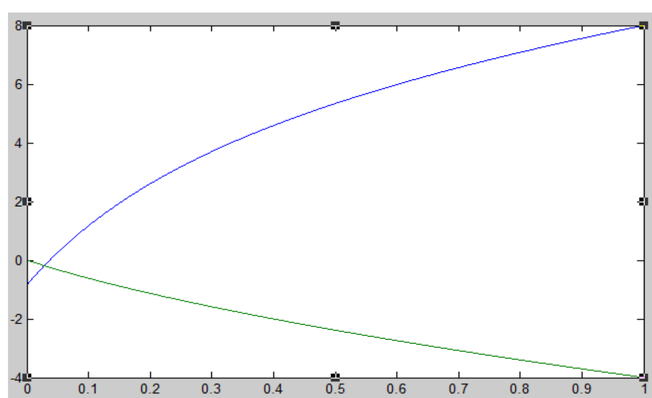

Figure 1.8:Variation of the LHS (blue color) and RHS (Green Color) inequation (1) and (2).This curve is plotted in case of l=4 and V=6.5. Also, the points of intersection represent the discrete modes of the waveguide.

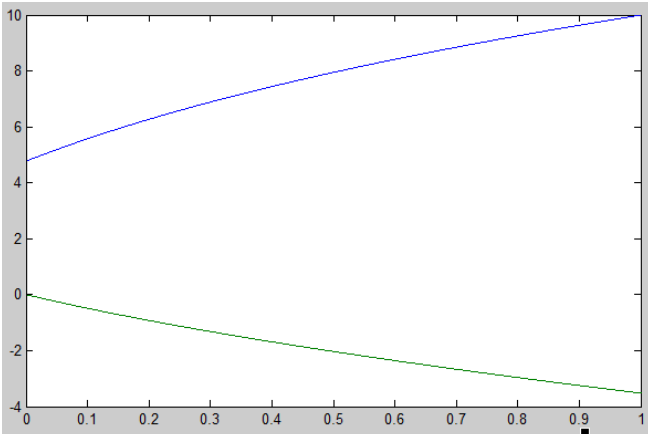

Figure 1.9: Variation of the LHS (blue color) and RHS (Green Color) in equation (1) and (2).This curve is plotted in case of l=5 and V=6.5. Also, the points of intersection represent the discrete modes of the waveguide.

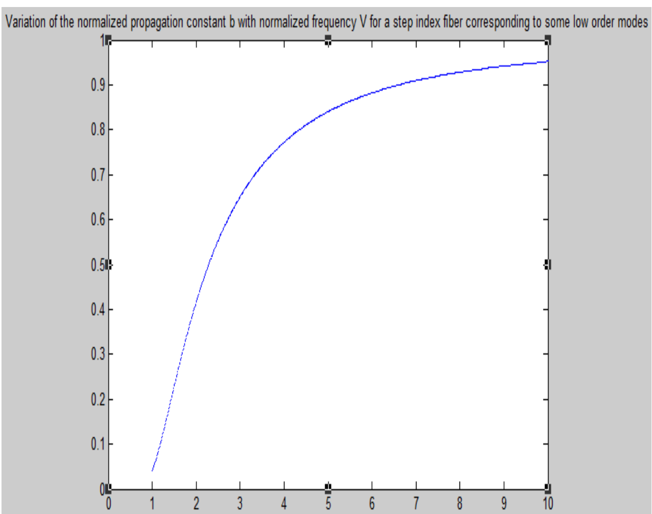

Figure 1.10:Variation of the normalized propagation constant b with normalized frequency for a step index fiber corresponding to some low order modes. The cutoff frequencies of LP_{2m} And L$P_{0,m+1}$

V. CONCLUSION

In this paper, I have used the Transfer matrix method and computed the propagation characteristic of Bragg fiber.

ACKNOWLEDGMENT

This work is supported by Krishna Institute of Engineering and Technology and Faculty of Engineering, Dr. A.P.J.Abdul Kalam Technical University, Lucknow.

REFERENCES

1) Prachi Sharma et al, "A Review of the Development in the Field of Fiber Optic Communication Systems", International Journal of Emerging Technology and Advanced Engineering, Vol. 3, no. 5, pp. 113-119, 2013.
2) http://www.optiwave.co.kr/product/broc hures.htm
3) Bijayananda Patnaik, Prasant Kumar Sahu," Long-Haul 64-Channel 10-Gbps DWDM System Design and Simulation in Presence of Optical Kerr's Effect",ICCCS'11, India, February-2011.
4) Bo-ning HU, Wang Jing, Wang Wei, Rui-mei Zhao," Analysis on Dispersion Compensation with DCF based on Optisystem". 2nd International Conference on Industrial and Information Systems, 2010.
5) Hill, K. O. and G. Meltz, "Fiber Bragg grating technology fundamentals and overview," J. Lightwave Technol., Vol. 15, 1263–1276, 1997.
6) Vengsarkar, A. M., etal., "Long-period fiber gratings as band-rejection filters," J. Lightwave Technol., Vol. 14, 58–65, 1996
7) Knight, J. C. and P. S. J. Russell, "Photonic crystal fibers: New way to guide light," Science, Vol. 296, 276–277, 2002.
8) Ibanescu, M., Y. Fink, S. Fan, E. L. Thomas, and L. D. Joannopoulos, "An all-dielectric coaxial waveguide," Science, Vol. 289, 415–419, 2000.
9) Hart, S. D., etal., "External reflection from omnidirectional dielectric mirror fibers," Science, Vol. 296, 510–513, 2002.
10) Kim, D. H. and J. U. Kang, "Sagnac loop interferometer based on polarization maintaining photonic crystal fiber with reduced temperature sensitivity," Opt. Express, Vol. 12, 4490–4495, 2004.
11) Konorov, S. O. and A. M. Zheltikov, "Photonic-crystal fiber as a multifunctional optical sensor and sample collector," Opt. Express, Vol. 13, 3454–3459, 2005.
12) Ouyang, G., Y. Xu, and A. Yariv, "Comparative study of air-core and coaxial Bragg fibres: Single-mode transmission and dispersion characteristics," Opt. Express, Vol. 9, 733–747, 2001
13) R P.Yeh, A. Yariv, and E. Marom, "Theory of Bragg fiber," J. Opt. Soc. Am. 68, 1196-1201 (1978).
14) S.D. Hart et al., "External Reflection from Omnidirectional Dielectric Mirror Fibers," Science 296, 510, (2002).
15) T. Katagiri, Y. Matsuura, and M. Miyagi, "Fabrication of silica-core photonic bandgap fiber with multilayer cladding," Optical Fiber Communication Conference 2004, WI1.
16) J. A. Monsoriu, E. Silvestre, A. Ferrando, P. Andrés, and Juan J. Miret, "High-index-core Bragg fibers: dispersion properties," Opt. Express 11, 1400-1405 (2003)